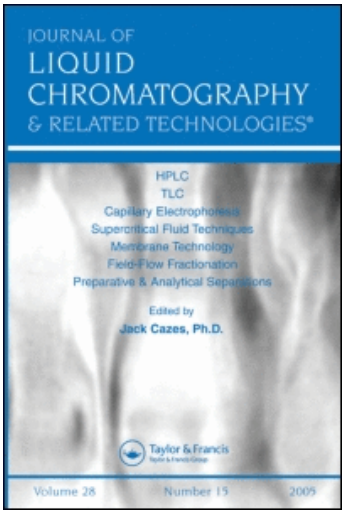

Journal of Liquid Chromatography & Related Technologies
Publication details, including instructions for authors and subscription information:
http://www.informaworld.com/smpp/title~content=t713597273

POLYMER ANALYSIS BY THERMAL FIELD-FLOW FRACTIONATION

Martin E. Schimpf[a]
[a] Department of Chemistry, Boise State University, Boise, ID, U.S.A.

Online publication date: 28 August 2002

To cite this Article Schimpf, Martin E.(2002) 'POLYMER ANALYSIS BY THERMAL FIELD-FLOW FRACTIONATION', Journal of Liquid Chromatography & Related Technologies, 25: 13, 2101 — 2134
To link to this Article: DOI: 10.1081/JLC-120013997
URL: http://dx.doi.org/10.1081/JLC-120013997

MARCEL DEKKER, INC. • 270 MADISON AVENUE • NEW YORK, NY 10016

JOURNAL OF LIQUID CHROMATOGRAPHY & RELATED TECHNOLOGIES
Vol. 25, Nos. 13–15, pp. 2101–2134, 2002

POLYMER ANALYSIS BY THERMAL FIELD-FLOW FRACTIONATION

Martin E. Schimpf

Department of Chemistry, Boise State University,
'Boise, ID 83725, USA
E-mail: mschimpf@chem.boise.state.edu

INTRODUCTION

Thermal field-flow fractionation (ThFFF) is an analytical technique used to separate lipophilic polymers according to differences in their molecular weight or chemical composition. When Giddings conceptualized FFF,[1] he was searching for a separation technique that could be more precisely modeled than the chromatographic techniques that were used at the time. His success in this regard forms the basis for one of the great strengths of FFF, which is its ability to directly calculate physicochemical parameters of analytes from their residence times in the separation channel. ThFFF, which is one of several FFF subtechniques, separates polymers by magnifying their differential response to a temperature gradient. The physicochemical parameter that quantifies the movement of polymers in a temperature gradient is the Soret coefficient (S), and can be calculated directly from a polymer's residence time in the ThFFF channel. From S, the molecular weight of the polymer can be calculated, provided the system is first calibrated using a well-characterized polymer standard of the same composition and the intrinsic viscosity of the component is known. Thus, from a single calibration run and a viscosity detector, ThFFF can be used to separate and characterize the molecular weight distribution (MWD) of polymer samples.

DOI: 10.1081/JLC-120013997
1082-6076 (Print); 1520-572X (Online)

www.dekker.com

Of course, MWDs can also be calculated from calibration curves that relate retention in the channel to molecular weight, similar to the procedure used in size exclusion chromatography.

In addition to its theoretical tractability, ThFFF has other advantages compared to chromatographic methods used for polymer analysis, such as size exclusion chromatography (SEC). But ThFFF also has certain disadvantages, and both are discussed in this paper, which focuses on the methodology used to apply ThFFF to polymer analysis. In many ways ThFFF and SEC are complimentary. Thus, for some applications only one of the two techniques can be used, while in other cases the choice between the two depends on the relative importance of competing factors discussed in this paper.

PRINCIPLES AND THEORY

Like chromatography, FFF relies on the differential migration of analyte components along the length of a conduit.[2] The difference between the two techniques lies in the method used to achieve that differential displacement. In chromatography, analytes either diffuse into or are forced through porous particles, whose surface area is purposefully large to maximize separation efficiency. The particles are packed into a column, and the turbulent flow of carrier liquid through the column follows a tortuous path. In FFF, the separation relies on the interaction of analyte with a force field, within a column that is both open and of well-defined geometry. Exposure of the analyte to surfaces are minimized and the flow of the carrier liquid is both viscous and laminar. In addition to the ability to precisely model such a system, these features make for a gentle separation, so that fragile molecules and molecular complexes can be characterized with little disruption.[3]

Besides its placid nature and theoretical tractability, another attractive feature of FFF is its applicability to a wide variety of materials and situations. By varying the nature of the applied field, materials are separated by different physical properties, including size, charge, density, and chemical composition. Furthermore, a single channel can be used for a wide variety of materials. For example, flow FFF has been used to separate materials ranging in size from 10^3 to 10^{18} g mol^{-1}.[4] This flexibility is tempered by the higher cost of the FFF channel compared to a chromatography column. However, the additional cost is less significant when a complete instrument is considered, and the lifetime of the FFF channel is virtually unlimited when properly used and maintained. For example, a number of channels in the author's laboratory continue to see heavy use after more than 10 years in operation.

The typical FFF channel has the geometry of a ribbon,[2] with a length of 30–50 cm, a breadth of 1–3 cm, and a thickness of 0.05–0.25 mm. The potential

gradient, or "field", is applied across the thin dimension (coordinate x). A stream of carrier liquid is introduced to the channel at one end and exits to a detector at the other. Because the channel has a high aspect ratio, this pressure-driven flow through the channel is laminar, with a well-defined velocity profile across the thin dimension. A mixture to be separated is injected into the flow path upstream from channel inlet, and subsequently transported to the outlet. While in transport, interactions with the applied field compress the sample against one wall (the accumulation wall), where the pressure driven velocity through the channel is reduced. The magnitude of a sample component's interaction with the field governs the extent to which its pressure-driven migration through the channel is retarded by its confinement to slower streamlines near the accumulation wall. In this way, differences in the field-induced transport across a few micrometers are magnified by differences in the pressure-driven transport of carrier liquid in a perpendicular dimension.

ThFFF instrumentation is similar to that for chromatography, consisting of a pump to drive the carrier liquid, an injector to introduce the sample, a separation channel, and a detector to monitor the channel effluent. A computer is used to control the magnitude of the applied field and to digitize and store the detector signal.

In the FFF experiment, the retention of a component is specified by its retention ratio R, which is calculated as $R = V^0/V_r$ where V^0 is the geometric (void) volume of the channel and V_r is the volume of carrier liquid required to flush the component through the channel. V_r is typically calculated from the time between sample injection and detection, and the flow rate through the channel. Note that a volume calculated in this way includes volumes between the injector and channel, and between the channel and detector. If these extra-channel volumes are significant, they should be subtracted before converting V_r to R, if physicochemical parameters are to be subsequently calculated from R, as outlined below.

Assuming a constant field and a parabolic velocity profile, R is related to the fundamental FFF retention parameter λ as follows:

$$R = 6\lambda[\coth(2\lambda)^{-1} - 2\lambda] \tag{1}$$

The dependence of λ on physicochemical parameters varies with the nature of the applied field; for ThFFF

$$\lambda = \frac{1}{wS(\mathrm{d}T/\mathrm{d}x)} = \frac{D}{D_T \Delta T} \tag{2}$$

where $\mathrm{d}T/\mathrm{d}x$ is the applied temperature gradient, which is well approximated by $\Delta T/w$, where ΔT is the difference in temperature between the hot and cold walls and w is the channel thickness. Thus, retention in ThFFF is governed by the Soret coefficient ($S = D_T/D$) and the difference in temperature between the hot and cold

walls. As $\lambda \to 0$, $R \to 0$ and $V_r \to \infty$, i.e., the analyte does not move through the channel. As $\lambda \to \infty$, $R \to 1$ ($V^0 = V_r$), and the analyte moves at the average velocity of the carrier liquid. With decreases in λ, the bracketed term in Eq. (1) approaches unity, so that for many applications the relationship between R and λ is described by the following simple equation:

$$R = 6\lambda \tag{3}$$

Equation (3) can be used in place of Eq. (2) with an error of less than 10% when $\lambda < 0.1$ ($R < 0.06$). For $\lambda < 0.2$ ($R < 0.7$), the equation $R = 6\lambda – 12\lambda^2$ can be used with an error of less than 2%. By convention, the thermal diffusion coefficient D_T is positive for diffusion in the x-direction, i.e., toward the accumulation wall, which is invariably the cold wall with polymers.

Strictly speaking, replacing dT/dx by $\Delta T/w$ in Eq. (2) is an approximation because dT/dx varies across the channel due to the temperature dependence of the carrier liquid's thermal conductivity. However, this effect is very small under normal operating conditions.[6] More significant is the effect of temperature on the viscosity of the carrier liquid, which skews the velocity profile toward the hot wall, and consequently affects the accuracy of Eq. (1). Various approaches have been used to account for the temperature dependence of the carrier liquid viscosity and thermal conductivity.[7,8] In one approach,[8] a flow-distortion parameter v is used to modify Eq. (1) as follows:

$$R = 6\lambda\left\{v + (1 - 6\lambda v)\left[\coth\left(\frac{1}{2\lambda}\right) - 2\lambda\right]\right\} \tag{4}$$

Precise values of v for 12 solvents, obtained by a complex numerical method, are contained in Reference (9). A procedure for estimating values of v from the temperature dependence of the carrier-liquid viscosity and thermal conductivity is given in Reference (10). However, for the routine analysis of polymers by ThFFF, Eq. (4) need not be used in place of Eq. (1) because molecular weight is typically related to R or λ through calibration plots, which incorporate secondary effects such as the temperature dependence of solvent parameters. Still, experience has shown that more flexible calibration curves can be made when Eq. (4) is used, as discussed later in this section.

The linear dependence of λ on ΔT^{-1} indicated in Eq. (2) was demonstrated early in the development of ThFFF.[11] This simple relationship facilitates tuning of the field in order to optimize the retention of individual samples. Equation (2) also indicates that the separation of components in a sample is based on differences in the ratio of their transport coefficients (D/D_T). Of the two transport coefficients, D_T is virtually independent of the molecular weight and branching configuration of a given polymer type, at least for random-coil homopolymers.[12,13] As a result, λ is a linear function of D for a given polymer-solvent system when the field (ΔT) is held constant, as illustrated in Fig. 1.

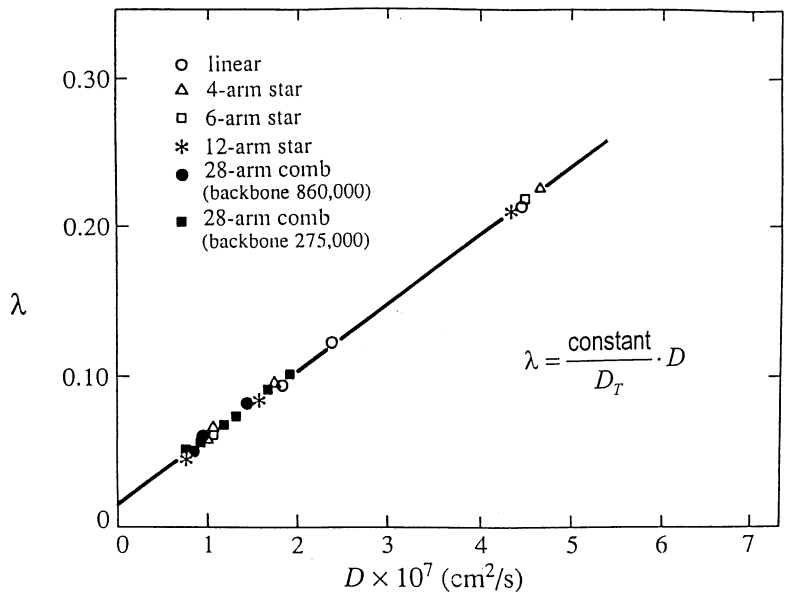

Figure 1. Dependence of retention parameter λ on diffusion coefficient D in ThFFF for polystyrene with different molecular weights and branching structures in ethylbenzene. The linearity of this plot, which was obtained using a fixed value of ΔT, demonstrates that D_T is constant, and therefore independent of molecular weight and branching configuration. Adapted with permission from reference 12. (Copyright 1986, American Chemical Society).

Like SEC, the separation of polymers according to molecular weight M in ThFFF is rooted in the dependence of D on M. That dependence is given by the following expression:[14]

$$D = \frac{kT}{6\pi\eta_o}\left(\frac{10\pi N_A}{3M[\eta]}\right)^{1/3} \tag{5}$$

where η_o is the viscosity of the solvent (carrier liquid), N_A is Avagadro's number, and $[\eta]$ is the intrinsic viscosity of the polymer. The relationship defined by Eq. (5) forms the basis for universal calibration in SEC,[15] where a single column that is calibrated in terms V_r vs. log $[(\eta)M]$ can be applied to a variety of different polymer types. Universal calibration is also applicable to ThFFF, and is discussed further in the section dealing with Applications and Method Selection: ThFFF vs. SEC.

The dependence of D on M is often expressed in the general form:

$$D = AM^b \tag{6}$$

where the coefficients A and b are constant for a given polymer-solvent system. Exponent b can be related to the Mark–Houwink coefficient a, which is the exponent that defines the dependence of $[\eta]$ on M in the Mark–Houwink equation:

$$[\eta] = KM^a \tag{7}$$

Thus, by combining Eqs. (5–7), we obtain the following relationship:

$$b = \frac{a+1}{3} \tag{8}$$

Since D_T is independent of M, one can write the ratio D/D_T that governs ThFFF retention in a form similar to Eq. (8):

$$D/D_T = BM^{b'} \tag{9}$$

(Note that $b' \neq b$ because polymers of different molecular weight are at slightly different temperatures in the channel, causing the dependence of D/D_T on M do be slightly different than the dependence of D on M.) Combining Eqs. (2) and (9) and rearranging yields the following dependence of retention on M:

$$\log \lambda \Delta T = \log B - b' \log M \tag{10}$$

A double logarithmic plot of $\lambda \Delta T$ vs. M for a set of linear polystyrene standards in the solvents tetrahydrofuran and ethylbenzene is illustrated[16] in Fig. 2. Since the data was gathered using a variety of field strengths, its linearity demonstrates the validity of Eq. (10). By calibrating ThFFF channels in terms of $\log \lambda \Delta T$ vs. $\log M$, the field strength can be changed to optimize the separation of a given sample without the need for re-calibration. It should be noted that values of λ used in this plot were calculated from experimentally measured values of R using Eq. (4). When Eq. (1) is used instead, such calibration plots may exhibit curvature, especially when they incorporate a broad range of retention levels (λ values). It should also be noted that calibration plots obtained in different solvents rarely coincide. In this case, they coincide because the dependence of D/D_T on M is nearly identical in the two solvents.

RESOLUTION AND FRACTIONATING POWER

In the separation of components by chromatography, the resolution index (R_s) is defined as the distance between two component peaks in the elution profile divided by the sum of their half-widths. The distance between peaks is a result of the selective separation process, while the half-width represents column dispersion, which reduces resolution because it causes the tails of the two peaks to approach one another, even as the peak centers remain a fixed distance

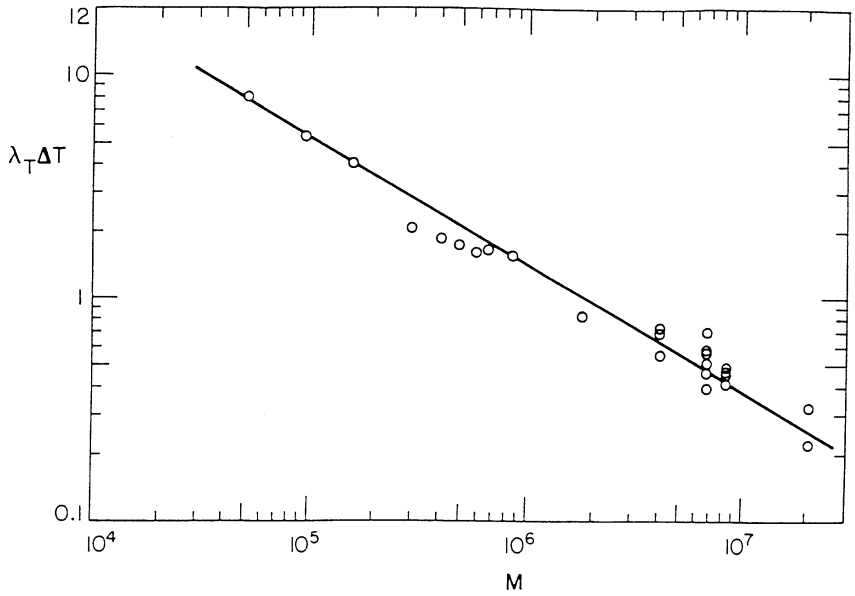

Figure 2. Plot of log $\lambda\Delta T$ vs. log M illustrating the validity of the calibration model expressed by Eq. (10). Note that the data from two different solvents form a single calibration line in this special case because the values of D_T are similar in the two solvents. Reprinted with permission from reference 16. (Copyright 1985, American Chemical Society).

apart. This model works well for quantifying separation efficiency in the case of two monodisperse components. For polymers, however, many partially separated molecular weight components are merged within a single peak, so that both selective separation and column dispersion contribute to the overall width of the peak. As a result, the resolution index has no practical utility.

For quantifying the resolution of polydisperse polymer samples, it is convenient to define the smallest relative molecular weight increment ($\Delta M/M$) that can be separated with unit resolution. This increment is termed the mass-based fractionating power F_m, and is related by the following equation to the number of theoretical plates N, which quantifies column dispersion, and the mass-based selectivity S_m, which quantifies the inherent ability of the technique to separate different molecular weight components:[17]

$$F_m = \left(\frac{M}{\Delta M}\right)_{R_s=1} = \frac{1}{4} N^{1/2} S_m \tag{11}$$

Parameters S_m and N are discussed individually below.

Selectivity

The inherent ability of an elution technique to separate different molecular weight components is defined by the change in some retention parameter with molecular weight. Based on the logarithmic form of Eq. (10), the change in λ with molecular weight can be defined as

$$S_{\max} = \left| \frac{\mathrm{d}(\log \lambda)}{\mathrm{d}(\log M)} \right| \tag{12}$$

Using this definition, the so-called maximum selectivity is constant for a given technique and polymer-solvent system. In ThFFF, $S_{\max}$ is equal to b', which is defined in Eq. (9). More relevant to the fractionating power, however, is the change in retention volume V_r with molecular weight:

$$S_m = \left| \frac{\mathrm{d}(\log V_r)}{\mathrm{d}(\log M)} \right| \tag{13}$$

This definition, which is termed the mass-based selectivity, is related to $S_{\max}$ in FFF by

$$S_m = \left| \frac{\mathrm{d}(\log V_r)}{\mathrm{d}(\log \lambda)} \right| \left| \frac{\mathrm{d}(\log \lambda)}{\mathrm{d}(\log M)} \right| = \left| \frac{\mathrm{d}(\log R)}{\mathrm{d}(\log \lambda)} \right| S_{\max} \tag{14}$$

The absolute value is used so that F_m increases directly with S_m as defined by Eq. (11). Differentiation of Eq. (1) and substitution into Eq. (14) yields the following general formula for S_m in FFF:[18]

$$\frac{S_m}{S_{\max}} = \left| 3\left(\frac{R}{36\lambda^2} + 1 - \frac{1}{R} \right) \right| \tag{15}$$

Figure 3 illustrates the dependence of S_m on R, expressed by Eq. (15) and plotted as the fraction of $S_{\max}$. Thus, S_m increases with the level of retention (i.e., as $R \to 0$) to a maximum value equal to $S_{\max}$ in the limit of infinite retention. This relationship is general to all FFF subtechniques. For random-coil polymers analyzed by ThFFF, values of S_m generally have a minimum value of 0.5 in a θ-solvent, and increase to a value near 0.7 with the goodness of the solvent. These values compare favorably to those in SEC, which are 0.2 or less.

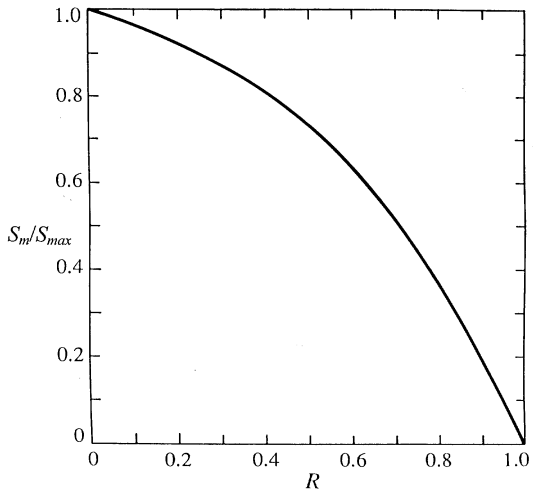

Figure 3. Dependence of the mass-based selectivity S_m on retention ratio R, plotted as a fraction of the maximum selectivity $S_{\max}$, which occurs in the limit of high retention ($R \to 0$). Reprinted with permission from reference 18. (Copyright 1991, John Wiley & Sons, Inc.).

Efficiency

The other component of fractionating power is separation efficiency, which is governed by column dispersion. Efficiency is often quantified by the number of theoretical plates, which can be defined as:[19]

$$N = \frac{V_r^{\,2}}{\sigma_{V_r}^2} \tag{16}$$

where $\sigma_{V_r}^2$ is the volume-based standard deviation in the elution profile of a monodisperse sample. Efficiency can also be expressed in terms of plate height H, which is related to N by

$$H = \frac{L}{N} = \frac{L\sigma_{V_r}^2}{V_r^{\,2}} \tag{17}$$

Here, L is the length of the separation device. The various contributions to peak dispersion, when expressed as plate heights, are additive. For example, the general expression for plate height in FFF is given by[20]

$$H = \frac{\chi w^2}{D}\langle v\rangle + H_P + \sum H_i \tag{18}$$

The first term on the right side of Eq. (18) represents the nonequilibrium contribution to plate height, which results from the stochastic movement of analyte molecules between flow steams of different velocity. Thus, even in a monodisperse sample, each molecule will take a different path in its movement along the separation axis. The resulting variance in the downstream velocity is reduced in molecules that diffuse more rapidly, and therefore undergo a greater statistical sampling of the different flow streams. The resulting variance is proportional to the average velocity $\langle v \rangle$ of the carrier liquid because residence time, and therefore statistical sampling, decreases as the flow rate is increased. The dependence of nonequilibrium plate height on the square of the channel thickness w results from the stochastic nature of diffusion and the effect of channel thickness on the distance over which molecules must diffuse in order to sample the different flow streams. Finally, the diffusion distance is smaller in sample zones that are compressed more by their interaction with the field, which is reflected in the dependence of H on the so-called nonequilibrium coefficient χ. Parameter χ has the following approximate dependence on retention parameter λ:[18]

$$\chi = 24\lambda^3(1 - 8\lambda + 12\lambda^2) \tag{19}$$

The nonequilibrium contribution to plate height is a form of resistance to mass transfer, which occurs in all forms of column chromatography. In chromatography, however, this contribution to dispersion is either independent or increases with retention.[19] In FFF, on the other hand, dispersion decreases rapidly with increases in the level of retention, i.e., as λ decreases [see Eqs. (18), (19) and Ref. (9)]. Thus, high levels of retention are beneficial to both selectivity and efficiency.

The second term (H_p) on the right side of Eq. (18) represents the dispersion due to polydispersity of the sample. This type of selective dispersion is favorable, since it results in the separation of different molecular weight components in the elution profile. For polymers, sample polydispersity μ is defined by the ratio of weight-average molecular weight M_w to number-average molecular weight M_n. The dependence of H_p on μ is well approximated by (20)

$$H_p = LS_m^2\left(1 - \frac{1}{\mu}\right) \tag{20}$$

The last term on the right side of Eq. (18) includes a variety of instrument-specific sources that are not easily modeled, including effects associated with sample injection, wall effects, and extra-column effects introduced in the connecting tubing and detector cell. These effects are generally negligible when the connecting tubing is minimized and sample relaxation techniques are used, as described in the Section on Sample Relaxation.

Longitudinal dispersion, which varies inversely with $\langle v \rangle$, is negligible in the separation of macromolecules, therefore, it is not included in Eq. (18). Thus, the

primary contribution to column dispersion in FFF is the nonequilibrium effect, which varies directly with the velocity of the carrier liquid and the square of the channel thickness. As a result, low flow rates and thin channels are used in situations where the fractionating power needs to be maximized. The tradeoff associated with lowering the flow rate is increased analysis time. Regarding channel thickness, the current practical limit is 53 μm (0.002 in) for commercial ThFFF channels. The effects of flow rate and channel thickness are discussed in more detail in the section on Optimization.

APPLICATIONS AND METHOD SELECTION: ThFFF VERSUS SEC

Lipophilic Polymers

ThFFF is best suited to lipophilic polymers. The technique does not work well for charged polymers because their response to the temperature gradient is insufficient. Although a variety of nonionic materials have been retained in water,[21] they are more efficiently separated by flow FFF.[22] Dextrans and other polysaccharides have been characterized by ThFFF using dimethyl sulfoxide (DMSO)[23] or a mixture of DMSO and water[24] as the carrier liquid, but DMSO is a particularly unpleasant solvent to work with.

Regarding the choice between FFF and chromatography, the preferred method depends on the priorities of the analyst, since each method has its own merits and limitations. One must first consider the molecular weight range to be analyzed. For oligomers and polymers having molecular weights less than $10^4\,\mathrm{g\,mol^{-1}}$, the use of SEC is almost mandatory, and certainly preferred. The lowest molecular weight that has been adequately retained for analysis by ThFFF using a commercially available channel is $2500\,\mathrm{g\,mol^{-1}}$.[25] The separation of several polystyrene components ranging from 2500 to $179{,}000\,\mathrm{g\,mol^{-1}}$ is illustrated in Fig. 4. The increase in peak width with retention in this fractrogram is not due to increased column dispersion, which decreases as discussed above. Nor is the increase in peak width due to an increase in the polydispersity index μ of the components. Part of the increase is due to an increase in selectivity S_m with retention, as illustrated in Fig. 3. However, there is an additional factor, which is relevant to the current comparison between FFF and SEC. Elution profiles are typically plotted as the detector signal vs. V_r (or retention time). However, $\mathrm{d}(\log V_r)/\mathrm{d}(\log M)$ is constant in FFF, which means that the spread in V_r for a given range in M (i.e., $\mathrm{d}V_r/\mathrm{d}M$) increases with M. As a result, peak width increases with retention time, even though column dispersion is actually decreasing.[10]

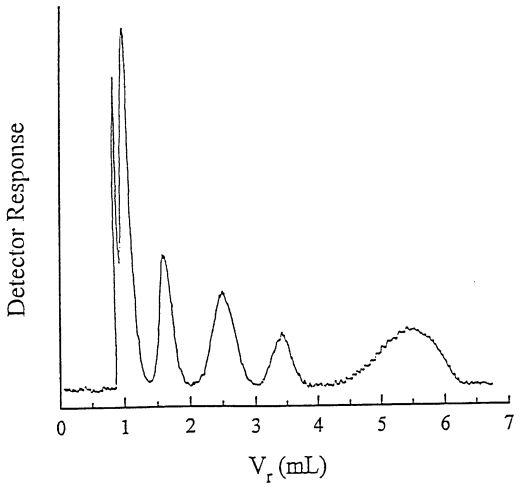

Figure 4. Separation of polystyrene in a mixture of 45 vol-% tetrahydrofuran in dodecane. From left to right, the first peak is the void peak, which is analogous to the permeation peak in SEC; successive peaks contain polystyrene standards of the following molecular weights, in thousands (k): 2.5 k, 20 k, 47 k, 97 k, and 179 k. Reprinted with permission from reference 25. (Copyright 1994, American Chemical Society).

In contrast to FFF, V_r scales with log D in SEC, therefore log M scales linearly with V_r[19] rather than log V_r. As a result, dV_r/dM is smaller compared to FFF, i.e., SEC is inherently less selective than ThFFF. Furthermore, the difference between SEC and ThFFF increases rapidly with M. On the other hand, ThFFF has fewer theoretical plates than SEC. The net result is that fractionating power in ThFFF exceeds that in SEC only for molecular weights above about $10^5\,g\,mol^{-1}$.[26] For ultra-high molecular weight polymers ($M > 10^6$), SEC becomes increasingly limited by shear-induced fragmentation of the chains as they travel through the packed bed under high pressure, and ThFFF is clearly superior.[27] This class of polymers is discussed in more detail in the following section of this paper. For molecular weights between 10^4 and $10^6\,g\,mol^{-1}$, neither SEC nor ThFFF has an overwhelming advantage, and the choice depends on additional factors. ThFFF has unique advantages for certain types of polymers, including high-temperature polymers, copolymers, gels and gel-containing polymers. These polymer types are discussed individually in subsequent sections.

For many homopolymers, both linear and branched, SEC is an easier technique to implement. One simply has to choose a column with the appropriate pore size, set up a calibration curve, and proceed to analyze a series of samples. If a separate measure of intrinsic viscosity is available, one can calibrate the column

with a series of polymer standards, e.g., polystyrene, and use the calibration plot to characterize the molecular weight of a variety of polymer types, provided the standards and samples have a similar conformation. In the case of calibration with polystyrene, for example, the polymers must assume a random coil conformation. This form of "universal" calibration in SEC is based on plots of log $[(\eta)M]$ vs. V_r and the relationship between $[\eta]M$ and D (Eq. 5), which governs the separation of polymers by SEC.

In general, ThFFF is more difficult to implement than SEC because there are more experimental factors that influence retention. While this adds flexibility to the technique, so that a single channel is used for many applications, it requires the user to understand the underlying principles of the separation. Only by understanding the principles can one avoid certain pitfalls in choosing the proper parameters for each application.

If the polymer analyst is willing to tackle the steep learning curve associated with ThFFF, there are some clear payoffs. As discussed above, ThFFF may yield a greater resolving power, depending on the polymer-solvent system and molecular weight. Another advantage lies in the fact that column dispersion in ThFFF conforms to a well-defined model, allowing its effect on the elution profile to be removed for highly precise information on polymer polydispersities.[28] Furthermore, for polydisperse polymers ($\mu > 1.2$), the effects of column dispersion are (unlike SEC) negligible, so that elution profiles can be converted directly into highly precise molecular weight distributions.[10] Finally, the peak capacity is greater in ThFFF compared to SEC. In ThFFF, V_r is unlimited in principle, although in practice it is limited to about 20 channel volumes. In SEC, V_r is limited at the high end by the permeation volume, which equals one column volume, and at the low end by the exclusion volume, which is defined by the column volume minus the pore volume.

As noted above, universal calibration with all its advantages is applicable to ThFFF as well as SEC. However, ThFFF requires knowledge of the thermal diffusion coefficient D_T for each polymer-solvent system under consideration. Fortunately, D_T is independent of M and branching configuration, so that only one value is required for each polymer type. A summary of D_T-values obtained by ThFFF is contained in Table 1. Such values are calculated using Eq. (2) after independent measurements of λ and D on an appropriate polymer standard.[12] D-values can be determined by dynamic light scattering or SEC (the latter is a secondary measurement).

Compared to SEC, universal calibration in ThFFF has the potential to be broader in scope, since the latter separation does not rely on packing materials, which vary from one batch to the next. Therefore, once the calibration constants are determined for a given polymer-solvent system, they should apply to all ThFFF channels that employ a given cold-wall temperature (T_c). A discussion of the progress made on integrating T_c into the calibration model is discussed in

Table 1. Summary of Known D_T Values of Polymers in Organic Solvents (D_T in $10^{-11}\,m^2\,s^{-1}\,K^{-1}$)

Solvent	PB	PI	PMMA	PαMS	PS	PTHF
Benzene		0.44	1.37	1.02	0.89	
Cyclohexane		0.20			0.66	0.28
Dioxane	0.18				0.42	< 0.1
Ethylacetate					1.16	
Ethylbenzene					0.95	
MEK					1.39	< 0.1
THF	0.25	0.57	1.33	1.27	1.00	0.52
Toluene	0.33	0.69	1.63	1.19	1.03	0.70

PB = polybutadiene; PI = polyisoprene; PMMA = polymethylmethacrylate; PαMS = poly(α-methyl)styrene; PS = polystyrene; PTHF = polytetrahydrofuran.

the section on Determination of Molecular Weight and Molecular Weight Distribution.

In summary, if the primary information desired is the average M for a lipophilic polymer sample, SEC is a simple and robust technique for molecular weights below $10^6\,g\,mol^{-1}$. However, for an analyst that requires the greatest possible precision on polymers with $M > 10^4\,g\,mol^{-1}$, or access to the ultra-high molecular weight range ($>10^6\,g\,mol^{-1}$), ThFFF has well-established advantages.

Ultra-High Molecular Weight Polymers, Gels, and Gel-Containing Polymers

The absence of shear forces in the FFF channel make it especially suited to ultra-high molecular weight polymers, gels, and colloids. In the analysis of poly(methyl methacrylate) (PMMA), for example, Lee compared the accuracy of SEC and ThFFF with and without the use of a MALS detector.[29] Without the MALS detector, SEC consistently underestimated *M.* With the absolute *M* detector, accuracy was still limited by the resolution of the separator because *M* is calculated with the assumption that each data slice is monodisperse. In either case, the superior resolution of ThFFF for high-*M* polymers made it the technique of choice.

ThFFF is also used to separate gel-containing polymers, including rubbers.[29–35] Since sample filtration is not required, microgels are not lost in the analysis. In fact, an estimate of the gel content is readily obtained. In one example, ThFFF was used to determine the difference between two acrylate elastomers that were manufactured by the same procedure but showed different mechanical properties.[32] Differences between the two elastomers could not be

distinguished using SEC, even in combination with viscometry or MALS. In another application,[33] ThFFF was used to monitor degradation of rubber during the mastication process. Workers at Goodyear Chemical routinely characterize emulsion styrene-butadiene copolymer blends by ThFFF,[34,35] citing its unique ability to detect components having molecular weights above $10^7\,\mathrm{g\,mol^{-1}}$.

Polysaccharides are another class of polymers that have proven difficult to separate by SEC. These materials have a wide range of industrial applications, from coating and packaging to plasma additives and blood substitutes. The physical, biological, and clinical properties of these materials vary with their molecular weight distribution (MWD), which is generally quite broad. It is difficult to prepare robust SEC packings that are capable of analyzing these fragile macromolecules without complications of sample adsorption, shear degradation and clogging of the column. Lou et al.[36] used ThFFF to fractionate a wide variety of polysaccharides according to their molecular weight.

It is important, when analyzing ultra-high molecular weight polymers by FFF, to use low flow rates[37] and polymer concentrations below the critical entanglement value[38] or else anomalous behavior will be observed due to viscous effects and shear-induced lift forces.[39] Flow rates below $0.2\,\mathrm{mL/min}$ should be sufficient in most cases, but the rate should be varied and the absence of any effect on the analysis should be verified.

High-Temperature Polymers

Polyolefins are particularly difficult polymers to separate because high temperatures ($>130^\circ$C) are required for their dissolution. At these temperatures, column packings used in SEC tend to degrade at an elevated rate. The robust ThFFF channel is more amenable to high temperatures. However, the cold wall temperature must be elevated to avoid precipitation of the polymer; therefore, cooling methods used in standard ThFFF channels cannot be used. Myers et al.[40] built a ThFFF channel specifically for high temperature applications. Heat is removed from the cold wall by the vaporization of deionized water that is preheated (120°C) before being rapidly pumped through cooling conduits in the cold wall. Dondi and coworkers have also developed a high-temperature ThFFF instrument, which they applied to polyethylene.[41] A commercial instrument may be available from Postnova Analytics (Salt Lake City, UT, USA) in the future.

Copolymers

Although the thermal diffusion coefficient D_T is independent of molecular weight, it varies with the composition of both polymer and solvent.[13] As a result,

polymer components that differ chemically can be resolved by ThFFF even when their molecular weights are identical.[42,43] Thus, two polymers that co-elute with SEC because their diffusion coefficients (or hydrodynamic volumes) are similar can often be resolved by ThFFF because they differ in chemical composition, and therefore have different D_T values.

Differences in D_T can also be used to separate copolymers according to composition. When the dependence of D_T on copolymer composition is known, the composition can be calculated using ThFFF retention data. Such is the case for random (statistical) copolymers, where D_T is a weighted-average of the D_T values of the homopolymer constituents, with the weighting factors being the mole-fractions of each component in the copolymer.[44] For example, a random copolymer composed of 75 mol-% styrene and 25 mol-% isoprene has a D_T-value of $0.75D_T^{\text{styrene}} + 0.25D_T^{\text{isoprene}}$, where D_T^{styrene} is the D_T value for pure polystyrene and D_T^{isoprene} is the D_T value for pure polyisoprene. By measuring the retention of a copolymer of unknown composition, its D/D_T value can be calculated using Eqs. (2) and (4). With an independent measure of D, a value for D_T can be calculated, and from D_T the copolymer composition. Although values of D_T for several polymers are listed in Table 1, for the best precision homopolymer D_T-values should be measured in the same channel as that used for copolymer analysis because D_T varies with cold-wall temperature. As was mentioned in the section dealing with Lipophilic Polymers, independent measures of D can be obtained by a variety of methods, including dynamic light scattering[45,46] and SEC.[47,48]

For characterizing the composition of block copolymers, it seems that one must be careful that the monomeric units (mers) are randomly oriented within the dissolved polymer-solvent sphere because D_T values are apparently influenced more strongly by mers located in the outer, free-draining region.[47] For linear-block copolymers, monomer segregation can be avoided with the use of a non-selective solvent, which is a solvent that is equally good for all copolymer components. However, in highly branched block copolymers, the segregation of mers is sometimes fixed by bonding constraints, so that even in a non-selective solvent D_T values fail to change in a predictable fashion with copolymer composition.[49]

ThFFF can also be combined with viscometry in order to determine both the average molecular weight and average composition of copolymers.[50] In the method, Eqs. (2) and (5) are combined with the linear dependence of D_T on composition to obtain the following equation for an *A-B* copolymer:

$$\frac{1}{\lambda} = \frac{6\pi\eta_o \Delta T}{kT_{cg}} \left(\frac{3[\eta]M}{10\pi N_A} \right)^{1/3} \left(D_T{}^B + \frac{X_A \Delta D_T}{100} \right) \tag{21}$$

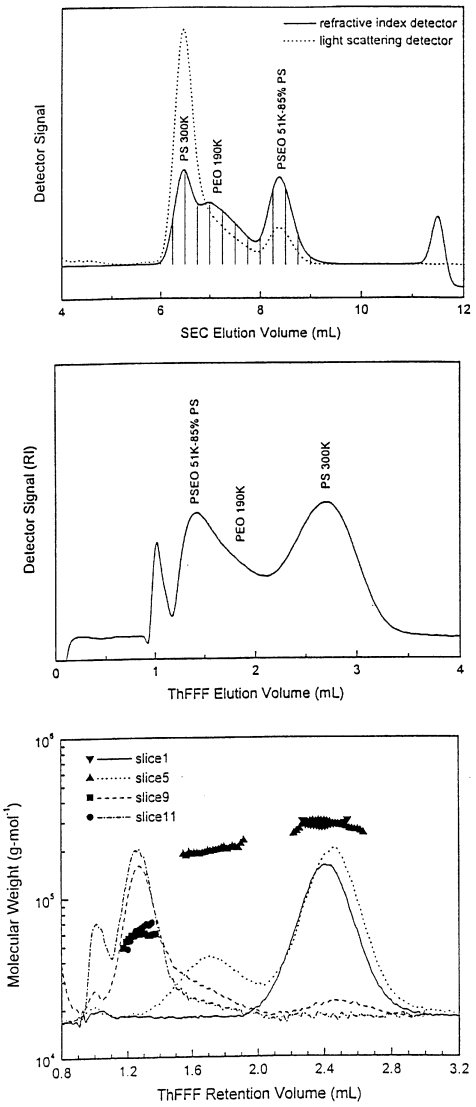

Figure 5. Cross-fractionation of a 3-component polymer mixture by SEC and ThFFF. The mixture could not be sufficiently resolved for characterization by either SEC (top) or ThFFF (middle) alone. Cross-fractionation of SEC elution slices (bottom) provided enough resolution to determine the molar mass of each component with a multi-angle light scattering detector (Dawn DSP, Wyatt Technology, Santa Barbara, CA). The composition of each component was determined from D and D_T values calculated from SEC and ThFFF retention volumes, respectively, as described in the text.

Here, D_T^B is the D_T-value for homopolymers of component B, X_A is the mole-fraction of component A in the copolymer, ΔD_T equals $D_T^B - D_T^A$, where D_T^A is the D_T values for a homopolymer of component A, and T_{cg} is the temperature at the center of gravity of the eluting copolymer zone. T_{cg} is well approximated by $T_{cg} = T_c + \lambda \Delta T$, where T_c is the temperature of the cold wall. By measuring λ and $[\eta]$ in two different solvents, a set of two equations can be solved for the two unknown parameters M and X_A in Eq. (21).

In some polymer mixtures, ThFFF is incapable of resolving all the components. For example, when the composition of a polydisperse copolymer changes with molecular weight, two components that differ in both molecular weight and composition can have the same D/D_T value, even though their individual values of D and D_T differ. Such components will co-elute in ThFFF. In such circumstances, the combination of SEC and ThFFF is extremely powerful. The components can first be separated according to differences in D using SEC, then fractions from the SEC column, which are homogeneous in D, can be further separated according to D_T by ThFFF.[51] Figure 5 illustrates such a combination applied to a polymer/copolymer mixture that neither SEC nor ThFFF alone could separate. By cross-fractionating the mixture, the three components were sufficiently resolved to determine both the molecular weight and composition of each component.

METHODOLOGY

Sample Relaxation

As the sample enters the channel, it relaxes into its steady-state concentration profile at the accumulation wall under the influence of the applied field. During this process, it experiences the full range of flow velocities that exist across the channel, which can lead to substantial zone broadening.[28] This additional source of dispersion can be minimized by stopping the axial flow of carrier liquid just after sample injection, so that the sample relaxes in the absence of such flow. Although the axial flow can be stopped by simply turning off the pump, the pressure pulse associated with restarting the pump can result in severe baseline disturbances. Therefore, it is better to interrupt the axial flow during sample relaxation by routing it around the channel with switching valves. In commercial instruments, these valves are precisely controlled by electronic switches and software that allows the user to vary the relaxation time.

Determination of Molecular Weight and Molecular Weight Distributions

The simplest calibration plots take the following form:

$$\log V_r = A' + S_m \log M \tag{22}$$

where A' and S_m are calibration constants for a given polymer-solvent system. Parameter S_m is the mass-based selectivity, which was defined in the section on Selectivity, Eq. (13). As outlined under Principles and Theory, retention theory predicts that such plots are linear (i.e., S_m is constant) only in the limit of high retention, where $R = V^0/V_r = 6\lambda$. At low-to-moderate levels of retention ($R > 0.1$), S_m changes rapidly with R, as illustrated in Fig. 3; therefore, calibration plots will not be linear. An alternate form of Eq. (22) allows for the use of low levels of retention without losing linearity in the calibration plot:[10]

$$\log(V_r - V^0) = A' + S_m \log M \tag{23}$$

Equation (23) allows retention to be calibrated over a wide range in molecular weight for a given polymer-solvent system without requiring the calculation of retention parameter λ. The problem remains, however, that neither Eq. (22) nor Eq. (23) allow for an adjustment in field strength, which is one of the great benefits of FFF because it allows the field to be optimized for each individual sample. In order to have a single calibration equation for different field strengths, one must incorporate the field strength by using Eq. (10).

It is worth noting that calibration equations are strictly valid only when the temperature of the cold wall (T_c) is carefully matched between calibration and analysis. Matching T_c is critical because the transport coefficients are temperature dependent. Problems can arise when the temperature of the liquid used for cooling the cold wall of the channel varies over time. For example, when the coolant is tap water, its temperature can change by several degrees over the course of one day, as well as with the change of seasons. In gathering the data illustrated in Fig. 2, which was used to verify the calibration equations in the form of Eq. (10), keeping T_c constant at 288K was critical for maintaining linearity in the plot. By using a coolant that is recirculated through a heater/chiller, it is easy to control T_c. Nevertheless, efforts have been made to incorporate the effect of T_c into the calibration equation. For example, in a detailed study of the effect of T_c on retention, Myers et al.[52,53] demonstrated that the dependence of D/D_T on T_c can be accurately modeled by the following equation:

$$\frac{D}{D_T} = \lambda \Delta T = a' {T_c}^m \tag{24}$$

The validity of this model is illustrated in Fig. 6 by the linearity in plots of log $\lambda\Delta T$ vs. log $T_c/298$. Based on Eq. (24), the following modified form of the calibration equation is proposed:

$$\log(\lambda\Delta T) = \phi + m\log\left(\frac{T_c}{298}\right) - n\log\left(\frac{M}{10^6}\right) \tag{25}$$

In order to utilize Eq. (25), a set of linear plots of log ($\lambda\Delta T$) vs. log $M/10^6$ is established for a given polymer-solvent system, with one plot being generated for each of several cold-wall temperatures. Such plots run parallel to one another with a slope equal to n, and with intercepts that equal [$\phi + m$ log ($T_c/298$)].

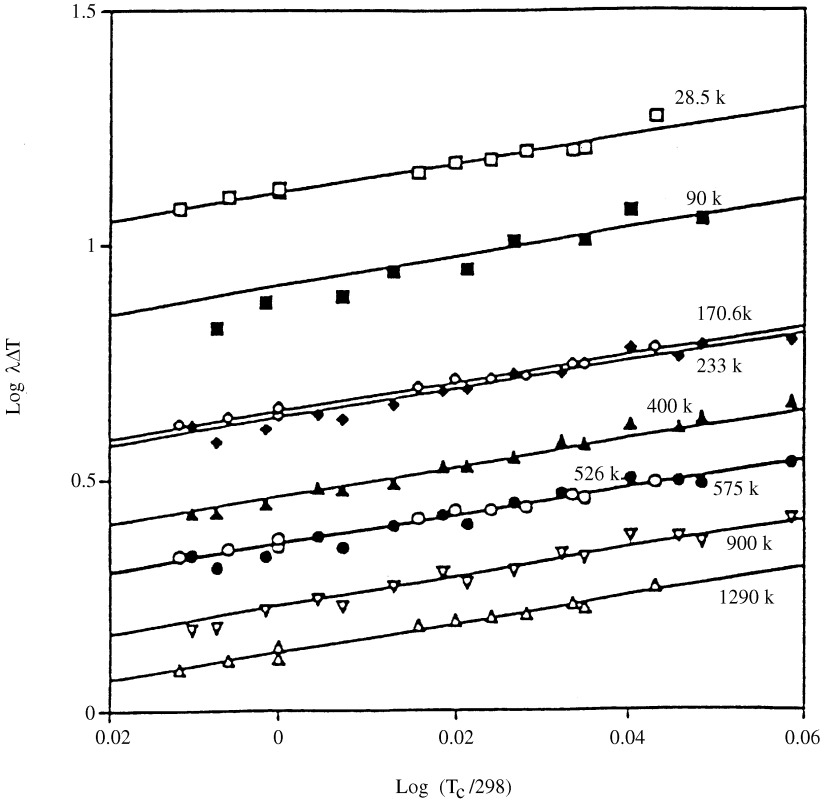

Figure 6. Plot of log $\lambda\Delta T$ vs. $T_c/298$ for polystyrene in tetrahydrofuran, illustrating the validity of the model expressed by Eq. (25). The data was gathered using a variety of different ThFFF channels. Values of ΔT ranged from 30–70K. Reprinted with permission from reference 52. (Copyright 1997, Dekker Publishing).

To obtain the values of ϕ and m, linear regression is performed on the intercept values as a function of $T_c/298$.[1]

When a mass-sensitive detector such as a refractometer or photometer is used, the weight-average molecular weight (M_w) of a polymer sample is calculated from the calibration equation using the value of V_r (or λ) that corresponds to the center of gravity of the elution profile. The center of gravity is defined by placing a vertical line through the elution profile such that the line bisects the profile into two halves of equal area. The intersection of this line with the elution-volume axis defines the weight-average V_r, which is converted to M_w through the calibration equation. If the elution profile has a Gaussian or other symmetrical shape, then the weight-average V_r is the value of V_r that corresponds to the peak of the elution profile.

In ThFFF, the shape of the elution profile is not significantly affected by column dispersion for polydisperse ($\mu > 1.2$) polymers, provided that low flow rates ($<0.4\,\text{mL/min}$) are used.[10] In such cases, accurate information on the MWD can be obtained directly from the elution profile. If a mass-sensitive detector is used, the signal (s) is linearly related to the mass of polymer in the eluting stream, and the number-average molecular weight (M_n) of the sample is calculated as:[10,54]

$$M_n = \frac{\sum s_i}{\sum s_i/M_i} \tag{26}$$

Here, the summation extends over small equal elements of elution volume from the beginning to the end of the elution profile. Thus, s_i is the detector signal of the i'th-digitized increment, and M_i is calculated from the associated value of V_r using the calibration equation. The weight-average molecular weight (M_w) is calculated as

$$M_w = \frac{\sum s_i M_i}{\sum s_i} \tag{27}$$

Polydispersity μ, defined as the ratio M_w/M_n, thus becomes

$$\mu = \frac{(\sum s_i M_i)(\sum s_i/M_i)}{(\sum s_i)^2} \tag{28}$$

A more detailed MWD can also be obtained from the elution profile. With a mass-sensitive detector, the elution profile is essentially a plot of the polymer concentration c (with units of mass/volume) in the eluting stream vs. V_r. In order

[1] T_c and M are divided by 298 and 10^6, respectively, to avoid large extrapolations in obtaining the various intercept values by regression techniques.

to obtain the mass-based MWD, $m(M)$, we need to transform this profile using the following equation:

$$m(M) = c(V_r)\frac{dV_r}{dM} \tag{29}$$

The normalized and digitized form of this equation is

$$m_i = \frac{s_i}{\sum s_i}\frac{\Delta V_r}{\Delta M_i} \tag{30}$$

where ΔV_r is the fixed elution volume element corresponding to one digitized interval. In the case of linear calibrations, as defined by Eqs. (22) and (23), $d(\log V_r)/d(\log M)$ is a constant equal to S_m, and Eq. (30) is more conveniently expressed in the following form:

$$m_i = \frac{s_i}{\sum s_i}\frac{M_i}{V_{r,i}}S_m \tag{31}$$

If needed, the differential number MWD can be obtained by dividing $m(M)$ by M:

$$n(M) = \frac{m(M)}{M} \tag{32}$$

For polymers with low polydispersity ($\mu < 1.2$), a detailed MWD is not needed, and simply calculating M_n and M_w from Eqs. (26) and (27) is generally adequate. However, the elution profile of such a narrow MWD is affected significantly by column dispersion, which must be accounted for in order to obtain the most accurate possible values of M_n and μ. Even the elution profile of more polydisperse samples ($\mu > 1.2$) can be affected by column dispersion if high flow rates (>0.4 mL/min) are used. Fortunately, column dispersion is well defined in ThFFF, and can be removed by one of two methods. For samples of low polydispersity, μ is well approximated by (28)

$$\mu = 1 + \frac{H_P}{LS_m{}^2} \tag{33}$$

where L is the channel length and H_P is the polydispersity contribution to plate height. H_P is obtained by plotting the experimental plate height as a function of flow rate. When the proper sample-relaxation technique is used, such plots are linear,[28] and the y-intercept is equivalent to H_P. Alternatively, H_P can be obtained by subtracting the nonequilibrium contribution to plate height (H_n) from the experimentally measured value. Methods for calculating H_n from well-established models of column dispersion in thermal FFF can be found in the literature.[10] Since the elution profile of samples with low polydispersity are generally symmetrical, M_w is calculated using the peak value of V_r in the

calibration equation, then Eq. (33) is used to calculate μ. Finally, M_n is calculated from $\mu = M_w/M_n$.

Samples with higher polydispersity do not generally yield symmetrical elution profiles. Moreover, a detailed MWD, either $m(M)$ or $n(M)$, is often desired. As mentioned above, column dispersion does not significantly affect the elution profile when low flow rates are used. Therefore, the elution profile is directly converted into a MWD by the procedures outlined above. If, on the other hand, fast flow rates are used to shorten analysis time, highly accurate MWDs can still be obtained by adjusting the elution profile to account for the effects of band broadening. A deconvolution algorithm that filters out column dispersion from the elution profile in ThFFF is described in the literature.[10]

Optimization

Optimizing a separation means either increasing the resolution of two or more components or reducing the analysis time. However, these are competing factors, thus that one cannot simply increase the flow rate of the carrier in an effort to speed the analysis without some sacrifice in fractionating power. FFF does have the advantage over chromatography that, within limits, the field and flow can be simultaneously increased to produce a faster analysis without a reduction in fractionating power, because column dispersion is reduced when the level of retention is increased. Ultimately, however, the field that can be applied is limited by the ability to remove heat from the cold wall. Furthermore, the level of retention is limited because of the potential for interactions with the accumulation wall as the sample is compressed into more concentrated zones at the wall. Therefore, a tradeoff exists between resolution and analysis time even in ThFFF, and optimization depends on the relative importance of these two competing factors.

Consider, for example, the quality control of a synthetic polymer, where the elution profile is examined in order to determine if the average molecular weight lies within a certain range. If a large number of samples must be run within a limited amount of time, it may be desirable to sacrifice some of the potential resolution in order to decrease analysis time. In this case, optimization means minimizing the analysis time so that just enough fractionating power is present that the difference between two critical molecular weight limits can be distinguished. This situation is in contrast to the potential need to characterize the distribution of M with the greatest possible precision, as in a polymer standard, for example. In the latter case, optimization means maximizing the fractionating power, with less concern for analysis time. Each of these situations is considered separately below.

Fractionating Power

The dominant contribution to column dispersion in FFF comes from nonequilibrium effects. This contribution, which arises from the resistance to mass transfer between different velocity sub-streams in the channel, is reduced for components with larger diffusion coefficients. Nonequilibrium dispersion is also reduced in thinner analyte zones, which corresponds to higher levels of retention (smaller λ). By integrating the well-defined model for nonequilibrium dispersion in FFF into the definition of fractionating power Eq. (11), one obtains the following expression (2):

$$F_m = S_m\left[\frac{bLD}{384\lambda^3 w\dot{V}}\right]^{1/2} \tag{34}$$

where b is the channel breadth and $\dot{V}$ is the volume-based axial flow rate.[2] According to Eq. (34), high levels of retention are beneficial to fractionating power for two reasons: S_m increases with retention, as discussed in Section 3.1, but more importantly, λ decreases with the level of retention. Channel thickness (w) is also an important factor, with thinner channels being more efficient. Note that while doubling the channel breadth (b) appears to double F_m, it also doubles the run time; thus, the same result can be achieved by cutting $\dot{V}$ in half. However, cutting w in half does not have the same effect as cutting $\dot{V}$ in half because the former decreases run time, while the latter increases run time. Thus, cutting w in half allows the user to simultaneously cut $\dot{V}$ in half, yielding a 4-fold increase in F_m with no increase in analysis time.

In contrast to low molecular weight samples, where λ can be reduced only so far before reaching limitations in the magnitude of the applied field, with high molecular weight samples one must be careful not to apply a field that is too large. Thus, while higher fields generally increase fractionating power, λ can only be reduced so far before the sample begins to interact with accumulation wall. Such interactions invalidate the relationships between retention and physicochemical parameters, whose measurement is often the goal of the FFF analysis. The value of λ where interactions begin to occur varies with the sample, but a general rule is to keep $\lambda > 0.008$ ($R > 0.05$). With this limit in mind, we can cast λ in terms of experimental variables that are used to manipulate the field strength, in order to consider the effect of such variables on F_m:

$$F_m = S_m\left[\frac{bLD_T{}^3}{384D^2}\right]^{1/2}\frac{(\Delta T)^{3/2}}{w^{1/2}\dot{V}^{1/2}} \tag{35}$$

[2]Although it appears that F_m increases with D, λ^3 increases with D^3, therefore F_m is inversely proportional to D^2.

Thus, fractionating power is enhanced by the use of large temperature drops, thin channels, and low axial flow rates.

Separation Time

In situations where sample throughput is a consideration, faster analysis times can be achieved at the expense of fractionating power and, consequently, at the expense of accuracy in the molecular weight distribution. Of course, the fractionating power cannot be completely disregarded, otherwise the separation will be lost completely. Therefore, we define the reduced fractionating power F'_m as the fractionating power per unit retention time (t_r), which can be obtained by dividing Eq. (35) by t_r:

$$F'_m = \frac{F_m}{t_r} = S_m \left[\frac{bLD}{384\lambda^3 w \dot{V} t_r^2} \right]^{1/2} \tag{36}$$

In the limit of high retention, we can use the approximation $R = 6\lambda$ and the dependence of retention time on flow rate to obtain the following relationship:

$$F'_m = S_m \left[\frac{3D\dot{V}}{32bL\lambda w^3} \right]^{1/2} \tag{37}$$

In contrast to F_m, which doesn't consider analysis time, F'_m increases with axial flow rate and decreases with channel length. F'_m also has a greater dependence on channel thickness and depends less on the retention parameter λ. By inserting the dependence of λ on experimental parameters, we obtain

$$F'_m = S_m \left[\frac{3D_T}{32bL} \right]^{1/2} \left[\frac{\dot{V}\Delta T}{w^3} \right]^{1/2} \tag{38}$$

As outlined in Section 3.2, column dispersion is well defined in ThFFF Eqs. (18–20). This means that if both analytical accuracy and analysis time are critical, the experiment can be sped along at the cost of increased column dispersion, which can later be removed mathematically from the elution profile[10,28] in order to increase the resolution. The drawback to such an approach is that programs to remove column dispersion from elution profiles are not commercially available.

Extra-Column Volume

Regardless of the application, optimization always includes minimizing the extra-column volume. Furthermore, when physicochemical parameters are being

calculated from measured levels of retention, optimization requires that the extra-column volume be known with precision, so that it can be accounted for in the calculation. Thus, all extra-column volumes should be subtracted from retention volumes, including the void volume if V^0 is obtained by measuring the retention volume of a sample that is not affected by the field.

Field Programming

In the separation of highly polydisperse materials, the field can be programmed in order to reduce analysis time without a great sacrifice in resolution. Programming the field is analogous to temperature programming in gas chromatography or gradient elution in liquid chromatography. By applying a high field initially, the lower-M components are adequately retained for their resolution and characterization. Once such components are eluted, maintaining the high field causes an unnecessary delay in the elution of higher-M components. Figure 7 illustrates the separation of components ranging in molecular weight from 9000 to 5,500,000 g mol^{-1} with a programmed field.

Several types of field-decay programs have been used,[55,57] including linear, exponential, and power programs. Commercial instruments employ a power program, where the proper choice of parameters allows the fractionating

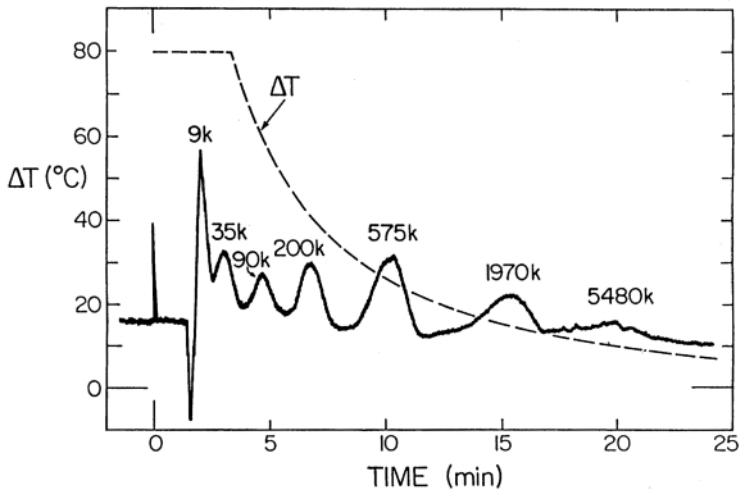

Figure 7. Separation of a seven-component mixture by ThFFF with field programming. Reprinted with permission from reference 57. (Copyright 1990, American Chemical Society).

power to remain almost constant throughout the run. In power programming, the field strength is held constant at S_0 for a period t_1 and then programmed according to the equation

$$S = S_0\left(\frac{t_1 - t_a}{t - t_a}\right)^p \tag{39}$$

where t_a is a second time parameter and p is a power greater than zero for a decay in field strength. The retention time (t_r') of a component can be approximated from its retention time $t_{r(0)}$ under conditions of a constant field S_0[2] by the following equation:

$$t_r' = (p+1)t_1\left(\frac{t_{r(0)}}{t_1}\right)^{1/(p+1)} \tag{40}$$

It can be shown[2] that the fractionating power of ThFFF is uniform over a wide range of retention levels when $p = 2$.

The user must be cautious in the use of programming because the field required to retain the lower molecular weight components will lead to significant compression of the higher molecular weight species against the accumulation wall.[58] High polymer concentrations often lead to nonideal behavior, such as molecular entanglement, gel formation, interaction with the accumulation wall, and under extreme circumstances, irreversible adsorption to the wall. The critical concentration c^*, where polymer solutions undergo an abrupt transition from dilute to semi-dilute behavior, is related to the radius of gyration $\langle r\rangle$ of the polymer and the density ρ of the solvent by the following equation:[59]

$$c^* = \frac{M}{\mathrm{N_A}\rho\langle r\rangle^3} \tag{41}$$

Although the effects of wall interactions can be accounted for by calibrating retention to M under identical conditions as those used for sample analysis, peak shape can deteriorate and precision will be reduced. The ragged profile of the high molecular weight component in Fig. 7 is likely due to wall such nonideal effects, which can be reduced by diluting the sample and further optimizing the field program.[57] The following equation can be used to approximate the maximum concentration that can be injected ($c_{\mathrm{inj,max}}$) without the polymer sample reaching the critical concentration upon compression by the field against the accumulation wall:

$$c_{\mathrm{inj,max}} \approx c^*\lambda \tag{42}$$

However, whenever high molecular weight materials are being analyzed, it is important to ensure the accurate determination of M-values by ensuring that such

values remain constant when the field strength is changed. If such values change with experimental conditions, then the sample should be diluted.

TRENDS IN DEVELOPMENT

The trend toward miniaturization of analytical-scale separation techniques has recently been extended to ThFFF.[60] The potential advantages include reduced solvent consumption, analysis time, and a smaller footprint. The power required to heat and cool the two opposing walls of the ThFFF channel also scale directly with the surface area of the walls, i.e., with channel breadth (b) and length (L). Scaling arguments also apply to channel efficiency. According to Eq. (35), for example, fractionating power scales inversely with the square root of the channel thickness. When separation time is considered, the reduced fractionating power Eq. (38) has an even stronger inverse dependence on channel thickness, as well as an inverse dependence on channel length.

There are some technical barriers to overcome before the potential benefits of miniaturization can be realized. Perhaps the most significant of these stems from the fact that retention in ThFFF scales directly with the temperature drop across the channel (ΔT) and not the temperature gradient (dT/dx) (see Eq. 2). Therefore, while reducing the channel thickness may increase the limiting value of dT/dx that can be realized, the value of ΔT required to achieve a level of retention comparable to the larger (thicker) channel remains the same. We have learned from working with standard ThFFF channels that as w is reduced, the maximum value of ΔT that can be achieved also decreases due to limits in the ability to remove heat from the cold wall. Currently, miniaturized ThFFF channels are made from microfabrication techniques that are based on silicon materials, which have poor thermal conductivity compared to the metals used in standard channels. The highest value of ΔT obtained thus far in a silicon channel is 4.8K.

Another difficulty with miniaturization is the need for detectors that are smaller but no less sensitive than those used in standard ThFFF instruments. On-channel detection is, in fact, preferred because the impact of external tubing on zone dispersion becomes significant as the volume of the separation channel is reduced. In standard channels, detection limit issues associated with the analysis of high-M and polydisperse polymers have been alleviated by the development of highly sensitive light scattering detectors, but miniature light scattering detectors are not available, and the potential of producing such devices is unclear.

Another development that may be on the horizon is the production of channels that are capable of continuous polymer fractionations. Vastamaki and coworkers[61] recently built a disk-shaped ThFFF channel with a rotating wall, in which separated components are collected continuously at the circumference of

the device. The device was used to separate polystyrene components in a cyclohexane carrier.

CONCLUSIONS

ThFFF has the demonstrated ability to separate and characterize lipophilic polymers with high accuracy and precision. The technique compares favorably with SEC in some cases, but not in others. While separation efficiencies are comparatively small in FFF, selectivity is quite high, and increases with molecular weight. As a result, the fractionating power is unmatched for polymers above $10^5\,\mathrm{g\,mol^{-1}}$. ThFFF really excels in the analysis of ultra-high molecular weight polymers ($M > 10^6\,\mathrm{g\,mol^{-1}}$), gels and colloids, as well as for the separation of polymer blends and copolymers, where SEC has very little selectivity.

A major advantage of ThFFF compared to SEC is that the retention mechanism is well modeled, so that transport coefficients and MWDs can be obtained with excellent accuracy and precision. The capability for programmed retention allows the separation to be optimized for each application, and allows highly polydisperse samples to be analyzed without sacrificing resolution at either end of the distribution.

The major drawback to ThFFF is the complexity that comes with its flexibility. Because there are several variables to control, the user must understand the underlying principles in order to develop a capability for applying the technique to new and different samples. Two of the more common mistakes by inexperienced users are

(1) the application fields that are too large and
(2) the preparation of samples that are too concentrated.

In the application to unknown but potentially high-M samples, a small field should be applied in the initial scouting run, and increased as necessary. Sample loads should be an order of magnitude lower than those typically used in SEC.

Another drawback to ThFFF is the relatively high cost of the separation channel compared to SEC columns. However, with proper maintenance, channel lifetimes are virtually unlimited.

When informative detectors are used, such as light scattering or viscometry, reliance on retention theory and calibration is reduced or even eliminated. In addition, the required level of expertise in FFF is reduced because optimization is less critical. Light scattering detectors also simplify the troubleshooting of problems associated with sample overloading. As a result of these and other advances, the application of FFF to polymer analysis continues to increase, competing channel manufacturers have recently appeared, and exciting new developments in miniaturization and continuous fractionation are on the horizon.

ACKNOWLEDGEMENTS

The author wishes to acknowledge the following sources of support for the development and application of FFF techniques: the National Science Foundation (grant CHE-9634195) and the Biomedical Research Infrastructure Network in Idaho (NIH-NCRR grant 1P20RR076454-01).

REFERENCES

1. Giddings, J.C. A New Separation Concept Based on a Coupling of Concentration and Flow Non Uniformities. Sep. Sci. **1966**, *1*, 123–125.
2. *FFF Handbook*; Schimpf, M.E., Caldwell, K.D., Giddings, J.C., Eds.; John Wiley: New York, 2000.
3. Gao, Y.S.; Caldwell, K.D.; Myers, M.N.; Giddings, J.C. Extension of Thermal FFF to Ultra High (20×10^6) Molecular Weight Polystyrenes. Macromol. **1985**, *18*, 1272–1277.
4. Ratanathanawongs, S.K.; Lee, I.; Giddings, J.C. Separation and Characterization of 0.01–5 μm Particles Using Flow FFF. In *Particle Size Distribution II. Assessment and Characterization*; Provder, T., Ed.; ACS Symposium Series No. 472; ACS Publications: Washington, D.C., 1991; Chapter 14, 217–228.
5. Grushka, E.; Caldwell, K.D.; Myers, M.N.; Giddings, J.C. Field-Flow Fractionation. Sep. Purif. Meth. **1973**, *2*, 127–510.
6. van Asten, A.C.; Boelens, H.F.M.; Kok, W.Th.; Poppe, H.; Williams, P.S.; Giddings, J.C. Temperature Dependence of Solvent Viscosity, Solvent Thermal Conductivity, and Soret Coefficient in Thermal FFF. Sep. Sci. Technol. **1994**, *29*, 513–533.
7. Gunderson, J.J.; Caldwell, K.D.; Giddings, J.C. Influence of Temperature Gradients on Velocity Profiles and Separation Parameters in Thermal FFF. Sep. Sci. Technol. **1984**, *19*, 831–847.
8. Martin, M. In *Advances in Chromatography*; Brown, P.R, Grushka, E., Eds.; Dekker: New York, 1998; Vol. 39, 1–138.
9. Belgaied, J.E.; Hoyos, M.; Martin, M. Velocity Profiles in Thermal FFF. J. Chromatogr. A **1994**, *678*, 85–96.
10. Schimpf, M.E.; Williams, P.S.; Giddings, J.C. Accurate Molecular Weight Distribution of Polymers Using Thermal FFF with Deconvolution to Remove System Dispersion. J. Appl. Polym. Sci. **1989**, *37*, 2059–2076.
11. Myers, M.N.; Caldwell, K.D.; Giddings, J.C. A Study of Retention in Thermal FFF. Sep. Sci. **1974**, *9*, 47–70.

12. Schimpf, M.E.; Giddings, J.C. Characterization of Thermal Diffusion in Polymer Solutions by Thermal FFF: Effects of Molecular Weight and Branching. Macromol. **1987**, *20*, 1561–1563.
13. Schimpf, M.E.; Giddings, J.C. Characterization of Thermal Diffusion in Polymer Solutions by Thermal FFF: Dependence on Polymer and Solvent Parameters. J. Polym. Sci.: Polym. Phys. Ed. **1989**, *27*, 1317–1332.
14. Rudin, A.; Johnston, H.K. J. Polym. Sci. B **1971**, *9*, 55.
15. Hamielec, A.E.; Ouano, A.C. Generalized Universal Molecular Weight Calibration Parameter in GPC. J. Liq. Chromatogr. **1978**, *1*, 111.
16. Gao, Y.S.; Caldwell, K.D.; Myers, M.N.; Giddings, J.C. Extension of Thermal FFF to Ultra-High Molecular Weight Polystyrenes. Macromol. **1985**, *18*, 1272.
17. Giddings, J.C.; Yoon, Y.H.; Myers, M.N. Evaluation and Comparison of Gel Permeation Chromatography and Thermal FFF for Polymer Separations. Anal. Chem. **1975**, *47*, 126–131.
18. Caldwell, K.D. In *Modern Methods of Polymer Characterization*; Barth, H.G., Mays, J.W., Eds.; John Wiley and Sons: New York, 1991.
19. Yau, W.W.; Kirkland, J.J.; Bly, D.D. *Modern Size Exclusion Chromatography*; Wiley-Interscience: New York, 1979; Chapter 3.
20. Smith, L.K.; Myers, M.N.; Giddings, J.C. Peak Broadening Factors in Thermal FFF. Anal. Chem. **1977**, *49*, 1750–1756.
21. Kirkland, J.J.; Yau, W.W. Thermal FFF of Water-Soluble Macromolecules. J. Chromatogr. **1986**, *553*, 95–107.
22. Giddings, J.C.; Benincasa, M.A.; Liu, K.K.; Li, P. Separation of Water Soluble Synthetic and Biological Macromolecules by Flow FFF. J. Liq. Chromatogr. **1992**, *15*, 1729–1747.
23. Lou, J.; Myers, M.N.; Giddings, J.C. Separation of Polysaccharides by Thermal FFF. J. Liq. Chromatogr. **1994**, *17*, 3239–3260.
24. Giddings, J.C.; Caldwell, K.D.; Myers, M.N. Thermal Diffusion in Eight Solvents by an Improved Thermal FFF Methodology. Macromol. **1976**, *9*, 106–112.
25. Rue, C.A.; Schimpf, M.E. Thermal Diffusion in Liquid Mixtures and Its Effect on Polymer Retention in Thermal FFF. Anal. Chem. **1994**, *66*, 4054–4062.
26. Gunderson, J.J.; Giddings, J.C. Comparison of Polymer Resolution in Thermal FFF and Size Exclusion Chromatography. Anal. Chim. Acta **1986**, *189*, 1–15.
27. Lee, S. Determination of Molecular Weight and Size of Ultrahigh Molecular Weight Polymers Using Thermal FFF and Light Scattering. In *Chromatographic Characterization of Polymers. Hyphenated and Multidimensional Techniques*; Provder, T., Barth, H.G., Urban, M.W., Eds.;

Advances in Chemistry Series 247; American Chemical Society: Washington, DC, 1995; 93–107.
28. Schimpf, M.E.; Myers, M.N.; Giddings, J.C. Determination of Polydispersity of Ultra-Narrow Polymer Fractions by Thermal FFF. J. Appl. Polym. Sci. **1987**, *31* (1), 117–135.
29. Lee, S. Gel Content Determination of Polymer Using Thermal FFF. In *Chromatography of Polymers: Characterization by SEC and FFF*; Provder, T., Ed.; ACS Symposium Series 521; ACS Publications: Washington, D.C., 1993; 77–89.
30. Antonietti, M.; Briel, A.; Tank, C. Chromatographic Characterization of Complex Polymer Systems with Thermal FFF. Acta Polymer. **1995**, *46*, 254–260.
31. Fulton, W.S.; Groves, S.A. Determination of the Molecular Architecture of Synthetic and Natural Rubber by the Use of Thermal FFF and Multi-Angle Laser Light Scattering. J. Nat. Rubb. Res. **1997**, *12*, 154–165.
32. Lee, S.; Molnar, A. Determination of Molecular Weight and Gel Content of Natural Rubber Using Thermal FFF. Macromol. **1995**, *28*, 6354–6356.
33. Lee, S.; Eum, C.H.; Plepys, A.R. Capability of Thermal FFF for Analysis of Processed Natural Rubber. Bull. Korean Chem. Soc. **2000**, *21*, 69–74.
34. Sibbald, M.; Lewandowski, L.; Mallamaci, M.; Johnson, E. Multidisciplinary Characterization of Novel Emulsion Polymers. Macromol. Symp. **2000**, *155*, 213–228.
35. Lewandowski, L.; Sibbald, M.S.; Johnson, E.; Mallamaci, M.P. New Emulsion SBR Technology: Part I: Raw Polymer Study. Rubber Chem. Technol. **2000**, *73*, 731–742.
36. Lou, J.; Myers, M.N.; Giddings, J.C. Separation of Polysaccharides by Thermal FFF. J. Liq. Chromatogr. **1994**, *17*, 3239–3260.
37. Janca, J.; Martin, M. Influence of Operational Parameters on Retention of Ultra-High Molecular Weight Polystyrenes in Thermal FFF. Chromatographia **1992**, *34*, 125.
38. Chubarova, E.V. Thermal FFF of Initially Dilute Polymer Solutions as a Shear Degradation Model. Scaling Model of Macromolecular Degradation at Concentrations Exceeding the Critical Entanglement Value. J. Macromol. Sci. Phys. **2000**, *B39*, 583–604.
39. Giddings, J.C.; Li, S.; Williams, P.S.; Schimpf, M.E. High-Speed Separation of Ultra-High Molecular Weight Polymers by Thermal/Hyperlayer FFF. Makromol. Chem. Rapid Commun. **1988**, *9*, 817–823.
40. Brimhall, S.L.; Myers, M.N.; Caldwell, K.D.; Giddings, J.C. High Temperature ThFFF for the Characterization of Polyethylene. Sep. Sci. Technol. **1981**, *6*, 671–689.

41. Pasti, L.; Roccasalvo, S.; Dondi, F.; Reschiglian, P. High Temperature Thermal FFF of Polyethylene and Polystyrene. J. Polym. Sci., Part B: Polym. Phys. **1995**, *33*, 1225–1234.
42. Gunderson, J.J.; Giddings, J.C. Chemical Composition and Molecular-Size Factors in Polymer Analysis by Thermal FFF and Size Exclusion Chromatography. Macromol. **1986**, *19*, 2618–2621.
43. Gunderson, J.J.; Giddings, J.C. Field-Flow Fractionation. In *Comprehensive Polymer Science, Vol. 1 Polymer Characterization*; Booth, C., Price, C., Eds.; Pergamon Press: Oxford, 1989; Chapter 14, 279–291.
44. Schimpf, M.E.; Wheeler, L.M.; Romeo, P.F. Copolymer Retention in Thermal Field-Flow Fractionation. In *Chromatography of Polymers*; Provder, T., Ed.; ACS Symposium Series 521; ACS Publications: Washington, D.C., 1992; Chapter 5, 63–76.
45. van Asten, A.C.; Kok, W.Th.; Tijssen, R.; Poppe, H. Study of Thermal Diffusion of Polybutadiene and Polytetrahydrofuran in Various Organic Solvents. J. Polym. Sci., Part B: Polym. Phys. **1996**, *34*, 297–308.
46. van Asten, A.C.; Kok, W. Th.; Tijssen, R.; Poppe, H. Characterization of Thermal Diffusion of Polystyrene in Binary Mixtures of THF/Dioxane and THF/Cyclohexane. J. Polym. Sci. Part B: Polym. Phys. **1996**, *34*, 283–295.
47. Schimpf, M.E.; Giddings, J.C. Characterization of Thermal Diffusion of Copolymers in Solution by Thermal FFF. J. Polym. Sci. Polym. Phys. Ed. **1990**, *28*, 2673–2680.
48. Nguyen, M.; Beckett, R.; Pille, L.; Solomon, D.H. Determination of Thermal Diffusion Coefficients for Polydisperse Polymers and Microgels by ThFFF and SEC-MALLS. Macromol. **1998**, *31*, 7003–7009.
49. Schimpf, M.E.; Rue, C.A.; Mercer, G.; Wheeler, L.M.; Romeo, P.F. Studies in the Thermal Diffusion of Copolymers. J. Coatings Technol. **1993**, *65*, 51–56.
50. Schimpf, M.E. Determination of Molecular Weight and Composition in Copolymers Using Thermal FFF Combined with Viscometry. In *Chromatographic Characterization of Polymers*; Provder, T., Barth, H.G., Urban, W., Eds.; Advances in Chemistry Series 247; ACS Publications: Washington, D.C., 1995; Chapter 14, 183–196.
51. Jeon, S.J.; Schimpf, M.E. Cross-Fractionation of Copolymers Using SEC and Thermal FFF for Determination of Molecular Weight and Composition. In *Chromatography of Polymers: Hyphenated and Multi-Dimensional Techniques*; Provder, T., Ed.; ACS Symposium Series No. 731; ACS Publications: Washington, D.C., 1999; Chapter 10, 141–161.
52. Myers, M.N.; Cao, W.; Chen, C.-L.; Kumar, V.; Giddings, J.C. Cold Wall Temperature Effects on Thermal FFF. J. Liq. Chrom. & Rel. Technol. **1997**, *20*, 2757–2775.

53. Cao, W.; Williams, P.S.; Myers, M.N.; Giddings, J.C. Thermal FFF Universal Calibration: Extension for Consideration of Variation of Cold Wall Temperature. Anal. Chem. **1999**, *71*, 1597–1609.
54. Tung, L.H. In *Polymer Fractionation*; Cantow, M.J.R., Ed.; Academic: New York, 1967.
55. Kirkland, J.J.; Rementer, S.W.; Yau, W.W. Molecular-Weight Distributions of Polymers by Thermal FFF With Exponential Temperature Programming. Anal. Chem. **1988**, *60*, 610–616.
56. Giddings, J.C.; Smith, L.K.; Myers, M.N. Programmed Thermal FFF. Anal. Chem. **1976**, *48*, 1587–1592.
57. Giddings, J.C.; Kumar, V.; Williams, P.S.; Myers, M.N. In *Polymer Characterization by Interdisciplinary Methods*; Craver, C.D., Provder, T., Eds.; ACS Advances in Chemistry Series No. 227; ACS Publications: Washington, DC, 1990; Chapter 1, 3–21.
58. Caldwell, K.D.; Brimhall, S.L.; Gao, Y.S.; Giddings, J.C. Sample Overloading Effects in Polymer Characterizations by Thermal FFF. J. Appl. Polym. Sci. **1988**, *36*, 703–719.
59. DeGennes, P.G. Dynamics of Entangled Polystyrene Solutions. I. Rouse Model. Macromol. **1976**, *9*, 587.
60. Edwards, T.L. A Microfabricated ThFFF System. Anal. Chem. **2002**, *74*, 1211–1216.
61. Vastamaki, P.; Jussila, M.; Riekkola, M.M. Development of Continuously Operating Two-Dimensional Thermal FFF Equipment. Sep. Sci. Technol. **2001**, *36*, 2535–2545.

Received May 13, 2002
Accepted May 27, 2002
Manuscript 5860